JOURNAL OF CATALYSIS 4, 469–479 (1965)

Kinetics and Mechanism of the Decomposition of Ammonia on Nonferrous Surfaces

A. J. NOZIK* AND D. W. BEHNKEN

From the Central Research Division, American Cyanamid Company, Stamford, Connecticut

Received October 1, 1964

The kinetics of the decomposition of ammonia on copper, Hastelloy C, and Inconel surfaces was determined, and the validity of three proposed kinetic models was tested with the aid of a computer. The data generally support the Ozaki-Taylor-Boudart mechanism for ammonia decomposition. However, surface heterogeneity is shown to have a significant effect upon the analysis.

INTRODUCTION

The kinetics and mechanism of the catalytic synthesis and decomposition of ammonia have been continuously investigated over the past 30 years. The bulk of these studies were conducted with ferrous catalysts, and the kinetics have, until recently, been dominated by the treatment presented by Temkin and Pyzhev (*1*) in 1940. This theory was based on the assumptions that:

(a) The rate-limiting step in the synthesis and decomposition of ammonia is the adsorption and desorption of nitrogen, and nitrogen atoms are the main adsorbed species on the catalyst surface.

(b) The catalyst surface is heterogeneous and the activation energies for adsorption and desorption vary linearly with coverage.

(c) The rates of adsorption and desorption of nitrogen atoms are described by the exponential-type Elovich expression.

The Temkin-Pyzhev mechanism can be summarized by the set of reactions

$$2\,NH_3 \rightleftharpoons 2\,(N)_a + 3\,H_2 \quad \text{(fast and equilibrated)} \quad (1)$$

$$2\,(N)_a \rightarrow N_2 \quad \text{(slow)} \quad (2)$$

where subscript a represents adsorbed species. The mathematical development of the theory leads to the following rate expression:

$$\frac{dP_{NH_3}}{dt} = k_s P_{N_2}\left[\frac{P_{H_2}^{\,3}}{P_{NH_3}^{\,2}}\right]^{\delta} - k_d\left[\frac{P_{NH_3}^{\,2}}{P_{H_2}^{\,3}}\right]^{1-\delta} \quad (3)$$

where δ is a parameter related to the heterogeneity of the surface, k_s and k_d are the rate constants for the synthesis and decomposition of ammonia, respectively, and P is partial pressure.

The Temkin-Pyzhev theory was fairly successful in describing the kinetics on ferrous catalysts, but there were several important discrepancies between theory and observation. The value of the parameter δ varied significantly among investigators; the theory predicted too strong a dependence of the rate on total pressure; and it also predicted an incorrect isotope effect when hydrogen was replaced by deuterium in the synthesis gas (*6*).

Several investigators have offered alternatives to the Temkin-Pyzhev theory. Horiuti (*2*), introducing his concept of stoichiometric number, proposed that the rate-limiting step in ammonia synthesis was the dehydrogenation of imine (NH) radicals. However, this mechanism led to a rate expression for ammonia decomposition which indicated an inhibitive effect of nitrogen (*2*c). This is contrary to results previously obtained by Emmett and Love (*3*, *4*), and to our own

* Present address: Department of Chemistry, Yale University, New Haven, Connecticut.

results, as we shall later describe. Also, Bokhoven, Gorgels, and Mars (*5*) measured the stoichiometric number to be one, which is in accordance with the proposition that nitrogen desorption and adsorption is rate-limiting.

Ozaki, Taylor, and Boudart (*6*) recently proposed another mechanism which retained some of the Temkin hypotheses, but accounted for the above-mentioned discrepancies. They assumed that the adsorption and desorption of nitrogen was still rate-limiting but that the surface was covered with (NH) radicals. The nitrogen atoms were thus adsorbing on the surface as (NH) radicals, said radicals being in equilibrium with NH_3 and H_2:

$$NH_3 \rightleftharpoons (NH)_a + H_2 \quad \text{(fast)} \quad (4)$$

$$2\,(NH)_a \rightarrow N_2 + 2\,H_a \quad \text{(slow)} \quad (5)$$

$$2\,H_a \rightleftharpoons H_2 \quad \text{(fast)} \quad (5a)$$

This mechanism led to the following rate expression:

$$\frac{dP_{NH_3}}{dt} = k_s P_{N_2} \left(\frac{P_{H_2}^2}{P_{NH_3}^2}\right)^{\delta} - k_d \left(\frac{P_{NH_3}^2}{P_{H_2}^2}\right)^{1-\delta} \quad (6)$$

Another interesting conjecture made by Ozaki, Taylor, and Boudart was that surface homogeneity or heterogeneity has no bearing on the kinetic analysis or the kinetic rate expression.

In this paper we shall examine the kinetics of the decomposition of ammonia on three nonferrous surfaces, and test the validity of the proposed models for the mechanism of ammonia decomposition on these surfaces. In addition, surface heterogeneity in the kinetic model will be examined.

Experimental

The data were obtained from an integral-flow-type reactor which is depicted in Fig. 1.

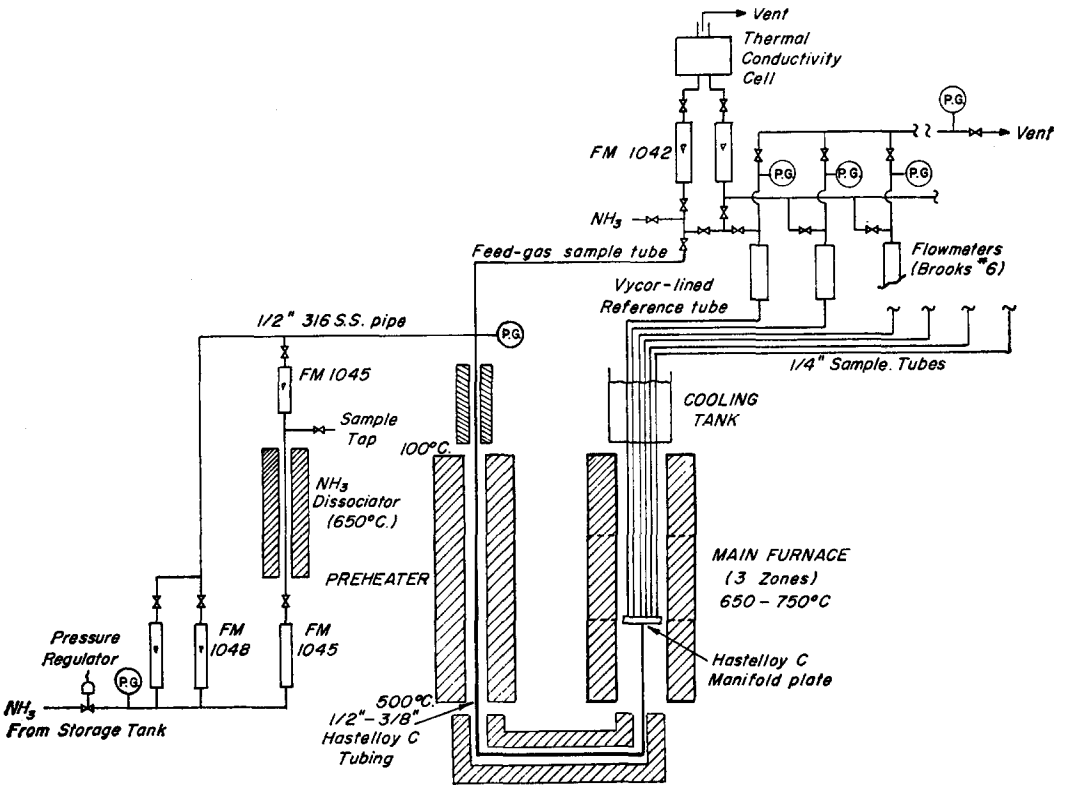

Fig. 1. Sketch of apparatus.

The materials studied were Hastelloy C, Inconel, and copper (lined on stainless steel).

The main section of the apparatus consisted of six parallel $\frac{1}{4}$-inch tubes located in the center of an electric furnace. Five tubes were made of the materials to be tested, and the sixth tube was a Hastelloy C Vycor-lined reference tube. The tubes extended 55 inches from a Hastelloy C manifold plate to the top of the furnace where they entered a water-quenched tank.

The temperature of the tubes was maintained and controlled at $\pm 1°C$ by a Pyrovane Controller. Six thermocouples were spot-welded along each tube, and measured its temperature profile.

The feed gas to the tube section was preheated in a separate preheat furnace, and also in the bottom section of the main furnace. The preheating sections were made of Hastelloy C to minimize precracking of the ammonia. The feed gas was distributed to all the tubes via a manifold plate, and the feed gas flow and pressure was controlled and maintained by Manostat rotameters and valves. The flow and pressure in each tube were also controlled by individual valves and rotameters.

The composition of the feed gas was fixed by mixing known quantities of pure NH_3 and decomposed NH_3 (75% H_2, 25% N_2). The decomposed NH_3 was obtained by passing some of the pure NH_3 through a dissociator (1-inch Inconel pipe packed with ammonia synthesis catalyst) maintained at 650°C. The NH_3 was obtained as liquid anhydrous ammonia from the Armour Industrial Company and was stored in a 1000 gallon tank (equipped with an electrically heated vaporizer and pressure regulator). The copper-lined stainless (314) duplex tube was obtained from the Texas Instrument Company, and the Hastelloy C and Inconel tubes were obtained from the Superior Tube Company.

The amount of ammonia decomposed in the preheaters and in each tube was determined by measuring the changes in hydrogen concentration. These analyses were performed by means of a thermal conductivity cell. To measure the ammonia precracking, the initial input feed was compared in the cell to the output from the Vycor reference tube. Since there is essentially no decomposition in the Vycor tube, the increase in hydrogen, as measured by the response from the thermal conductivity cell, is due to decomposition occurring in the preheating sections. By comparing the output from each tube to the output from the Vycor tube, the degree of decomposition in each tube was determined. The cell was calibrated at various levels of hydrogen concentration.

The total flow in each tube was about 60–70 g moles/hr. This corresponded to a Reynolds number of about 2400. Calculations* indicated that diffusion effects under the conditions of the experiments were not significant, and not controlling. This was also verified experimentally by several experiments at higher flow rates (120–140 g moles/hr). The decomposition rate, and the kinetic parameters were independent of flow rate.

Sample History

Previous experience had shown that the kinetic characteristics of metals and alloys change significantly with time. These changes are associated with surface nitriding, phase changes, precipitation, recrystallization, etc. Therefore, the sample tubes were continuously exposed to the ammonia environment at 700°C for 3000 hr before the data were taken. The decomposition rate for each tube, except for copper, was constant after this time.

Examination of photomicrographs indicated that the copper tube surface had undergone severe roughening and pitting. This roughening, and the resultant increase in surface area, accounts for the continued increase in the ammonia decomposition rate in the copper tube with time. However, the data were taken over a short enough time period to minimize the effect of this drift in rate on the kinetic analysis.

Analysis of Data

A test for the validity of the proposed kinetic models for ammonia decomposition

* Mass transfer coefficients for hydrogen were in the order of 400–500 g/moles/hr cm^2 atm, and the concentration gradients were in the order of 5%.

is to independently determine the partial pressure exponents of the rate expression

$$r_d = -Ce^{-E/RT}P_{NH_3}{}^nP_{H_2}{}^{-m} \quad (7)$$

where r_d is the decomposition rate, g moles/hr cm^2, C is the pre-exponential factor, g moles (atm)$^{m-n}$/hr cm^2, and E is the activation energy for decomposition, cal/g mole. The Temkin-Pyzhev model predicts a m/n value of 3/2 (*1*), and the Ozaki-Taylor-Boudart model predicts a m/n value of 1 (*6*).

Also, a determination of the effect of excess nitrogen on the rate of ammonia decomposition would check the Horiuti model, which predicts an inhibitive effect of nitrogen (*2*c, *4*).

Equation (7), written in terms of the experimental configuration, becomes

$$r_d = \frac{1}{2\pi r'}\frac{dA'}{dl} = -Ce^{-E/RT(l)}[P_{NH_3}(A')]^n[P_{H_2}(A')]^{-m} \quad (8)$$

where A' is the ammonia flow rate in g moles/hr, r' the tube radius, and l the tube length in centimeters, and $T(l)$ is the temperature profile along the tube, in °K/cm. Also, from the stoichiometry of the decomposition

$$P_{H_2}(A') = P_0\left\{\frac{B'(0) - \frac{3}{2}[A'(l) - A'(0)]}{B'(0) + C'(0) + 2A'(0) - A'(l)}\right\} \quad (9)$$

$$P_{NH_3}(A') = P_0\left\{\frac{A'(l)}{B'(0) + C'(0) + 2A'(0) - A'(l)}\right\} \quad (10)$$

where $A'(0)$, $B'(0)$, $C'(0)$ are the input molar flow rates to the tube of ammonia, hydrogen, and nitrogen, respectively; $A'(l)$ is the ammonia flow rate as a function of length in g moles/hr, and P_0 is the total pressure.

The kinetic parameters C, E, m, and n were estimated by least squares using a computer to perform the required numerical integrations and iterative nonlinear estimation procedure. The experiments performed to evaluate the kinetic parameters were an approximation to a two-level factorial design, with three intermediate (center) points, in the variables $1/T$, ln $P_{NH_3}(A')$, and ln $P_{H_2}(A')$. The actual independent variables which were controlled in the experiment were temperature (650–750°C), hydrogen concentration (3–12%), and total pressure (10–30 psig). Since two replicates were obtained, a total of 22 observations were made at the various combinations of variable levels. The data obtained from each experiment consisted of, (a) the initial flow rates of NH_3, H_2, and N_2 to the unit; (b) X_1, the increase in the mole fraction of H_2 due to ammonia decomposition between the feed point and the entrance to the tubes; (c) X_{2-i}, the increase in the mole fraction of H_2 due to ammonia decomposition in the ith tube; (d) the temperature profile along each tube as measured by six fixed thermocouples; and (e) flow and pressure measurements at the exit of each tube, as well as at the feed point of the unit. These data, together with X_1, allowed the computer to calculate the flow rates at the entrances to each tube $[A'(0)_i, B'(0)_i, C'(0)_i]$, the average total pressure in each tube, and the partial pressures of each component as a function of length.

The parameters of the rate expression were then determined in a two-stage procedure. First, they were approximated by assuming a linear or differential change in ammonia partial pressure in the tubes. That is

$$\Delta A'/2\pi r\Delta l = -Ce^{-E/R\bar{T}}[\bar{P}_{NH_3}(A')]^n[\bar{P}_{H_2}(A')]^{-m} \quad (11)$$

or

$$\ln(-\Delta A'/2\pi r\Delta l) = \ln C - (E/R\bar{T}) + n\ln[\bar{P}_{NH_3}(A')] - m\ln[\bar{P}_{H_2}(A')] \quad (12)$$

where

$$\bar{T} = \int_0^L T(l)dl/L \quad (13)$$

$$\bar{P}_{NH_3}(A') = \tfrac{1}{2}\{P_{NH_3}[A'(0)] + P_{NH_3}[A'(L)]\}. \quad (14)$$

$$\bar{P}_{H_2}(A') = \tfrac{1}{2}\{P_{H_2}[A'(0)] + P_{H_2}[A'(L)]\}. \quad (15)$$

Since Eq. (12) is linear in the parameters ln C, E, m, n, a standard linear least-squares procedure was used to determine them (*7*).

The computer, given a set of first guesses for the parameters, the boundary conditions $[A'(0), B'(0), C'(0)]$, P_0, and the temperature profile $[T(l)]$, next numerically integrates Eq. (8) using a Runge-Kutta procedure (*8*). An interpolation scheme provides values of T for any l, and a graph of A', B', and C' versus l is actually provided by the program.

The integration proceeds from the calculated boundary conditions at $l = 0$ to the terminal flow rates at $l = L$. Given the value of $A'(L)$, it is then possible to calculate the increase in mole fraction of hydrogen $\hat{X}_{2i}$

$$\hat{X}_{2i} = \frac{B'(0) + \frac{3}{2}[A'(0) - A'(L)]}{A'(0) + B'(0) + C'(0) + [A'(0) - A'(L)]} - \frac{B'(0)}{A'(0) + B'(0) + C'(0)} \quad (16)$$

where the supercarat ($\hat{}$) indicates calculated values. The experimentally observed increase in hydrogen mole fraction, X_{2i}, was then compared to the calculated value in a nonlinear least-squares procedure to determine the appropriateness of the estimated parameter values

$$S_i^2(C_i, E_i, m_i, n_i) = \sum_{j=1}^{22} (\ln X_{2-ij} - \ln \hat{X}_{2-ij})^2 \quad (17)$$

The index j runs over the 22 observations, while the index i refers to each of the six tubes. The logarithmic transformation was used to obtain a more uniform variance structure in the observations, since the per cent error in X_2 is more or less constant.

Parameters were sought by the computer which would minimize the residual sum of squares function, Eq. (17). A Gauss iterative procedure was used which is based on a series of linear approximations (*9*).

Results

The best estimates of the parameters, their 95% confidence intervals, and the mean and residual sums of squared deviation, are presented in Table 1. The confidence intervals for the copper parameters were not determined because of the poor fit of the copper data.

The estimated values of m and n are nearly equal for all the tubes. Statistical tests showed that the data were strongly concordant with the hypothesis that $m = n$ (t values of 0.14, 0.34, 0.42, and 1.2 were obtained in approximate t tests of the hypothesis $m = n$ for tubes 3, 4, 5, and 6 respectively). The parameters were then estimated for the model

$$r_d = -Ce^{-E/RT}(P_{NH_3}/P_{H_2})^m \quad (18)$$

and the results are presented in Table 2. As seen in this table, the fit of the data to Eq. (18) is as good as the fit to Eq. (7).

The individual marginal confidence in-

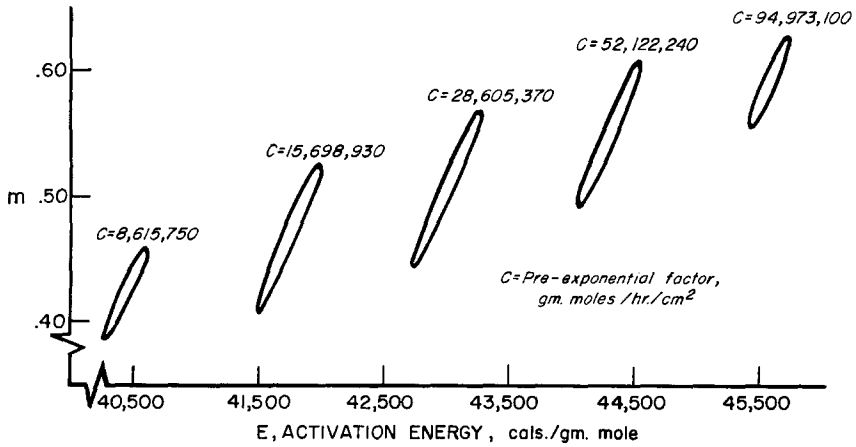

FIG. 2. Ninety-five per cent confidence region for Hastelloy C kinetic parameters.

TABLE 1

ESTIMATES AND 95% CONFIDENCE INTERVALS FOR KINETIC PARAMETERS OF EQ. (7)

Parameters	Hastelloy C Tube 3			Inconel Tube 4			Hastelloy C Tube 5			Inconel Tube 6			Copper Tube 2
	Lower limit	Estimate	Upper limit	Lower limit	Estimate	Upper limit	Lower limit	Estimate	Upper limit	Lower limit	Estimate	Upper limit	Estimate
$C \times 10^{-6}$, g moles $\frac{(\text{atm})^{m-n}}{\text{hr/cm}^2}$	10.20	27.65	97.28	3.14	9.44	36.26	10.26	47.24	214.79	5.59	15.09	40.65	0.2664
E, $\frac{\text{cal}}{\text{g mole}}$	40 930	42 970	45 010	37 160	39 280	41 400	41 790	44 220	46 650	39 320	40 980	42 650	42 550
m	0.4213	0.5033	0.5853	0.4542	0.5413	0.6284	0.4699	0.5701	0.6703	0.5066	0.5753	0.6440	1.050
n	0.3845	0.5258	0.6671	0.4088	0.5335	0.6582	0.4304	0.6045	0.7786	0.5288	0.6368	0.7448	1.049
Residual sum of squares		0.0428			0.0245			0.0638			0.0203		2.33
Residual mean square		0.00238			0.00136			0.00354			0.00113		0.129

TABLE 2

ESTIMATES AND 95% CONFIDENCE INTERVALS FOR KINETIC PARAMETERS OF EQ. (18)

Tube	Tube 3			Tube 4			Tube 5			Tube 6		
	Lower limit	Estimate	Upper limit	Lower limit	Estimate	Upper limit	Lower limit	Estimate	Upper limit	Lower limit	Estimate	Upper limit
$C \times 10^{-6}$, $\frac{\text{g moles}}{\text{hr/cm}^2}$	11.26	28.61	72.66	3.90	10.55	28.54	16.18	49.41	150.93	7.39	16.56	37.14
E, $\frac{\text{cal}}{\text{g mole}}$	41 020	43 020	45 020	37 170	39 270	41 360	41 900	44 290	46 690	39 400	41 110	42 820
m	0.4281	0.5069	0.5856	0.4553	0.5399	0.6245	0.4792	0.5765	0.6737	0.5168	0.5868	0.6569
Residual sum of squares		0.0430			0.0245			0.06513			0.02215	
Residual mean square		0.00226			0.00129			0.00343			0.00117	

tervals given in Tables 1 and 2 do not completely describe what has actually been learned about the parameters. Since the estimates are highly correlated, it is necessary to look at the joint confidence region for the parameters. This is approximated by an ellipsoid in the space of the parameters, with its center at the least-squares estimate and defined so that the probability is 0.95 that the region contains the true parameter values. The contours of such a region have been graphed for the Tube 3 (Hastelloy C) parameters (Fig. 2). The high correlation between the estimates C and E ($\rho = 0.99$) can be seen by noting that large variations in C from the least-squares estimate are consistent with the data as long as corresponding changes in E are made to keep the parameter point within the flattened cigar-shaped confidence region. While the range of likely parameter values is large (especially C), this is compensated for by the fact that the proportion of parameter space volume falling within these ranges occupied by *compatible* parameter values (points inside the confidence region) is quite small. When the estimated parameters are used to predict instantaneous rates (via the differential equation) the high correlations tend to have compensating effects on the variance of the predicted rate. This is apparent in the 95% confidence intervals for the instantaneous rates based on Eq. (18). These data are shown in Table 3, and indicate that the instantaneous rates are predicted within 4–8%.

TABLE 3
ESTIMATED INSTANTANEOUS DECOMPOSITION RATES[a] AND THEIR 95% CONFIDENCE INTERVAL

Tube	Lower limit	Estimate	Upper limit
2	—	0.00066	—
3	0.01757	0.01841	0.01929
4	0.04701	0.04079	0.05487
5	0.01793	0.01907	0.02029
6	0.03217	0.03398	0.03590

[a] $dA/2\pi rdl$, evaluated at 700°C, 10% H_2, 35 psia, g moles NH_3/hr/cm^2.

The instantaneous decomposition rates for the two Hastelloy C tubes are comparable. However, the decomposition rates for the two Inconel tubes differ by about 37%. This difference is attributed to the variation in grain size between the Inconel tubes. Tube 4, which was observed to have the finer grain size, had a higher catalytic activity. The grain sizes of the Hastelloy C tubes were found to be similar.

KINETIC MODELS

The data for Hastelloy C and Inconel support the Ozaki-Taylor-Boudart model for ammonia decomposition. However, for copper, the fit of the data to Eq. (8) is not very good. Although m/n is about 1, the residual sum of squares is 2.3 compared to about 0.05 for the other tubes. Although part of this large residual is due to the lower conversions in the copper tube, and its larger attendant relative error, the fit is significantly poorer than for Hastelloy C or Inconel.

According to Ozaki, Taylor, and Boudart, the nature of the catalyst surface is irrelevant to the kinetic analysis. This is true for the kinetics of ammonia synthesis, as they have shown. However, examination of the kinetics of ammonia decomposition indicates that the rate expression is dependent on whether a homogeneous or heterogeneous surface is assumed. The data for copper was thus examined on the basis of a homogeneous surface.

HETEROGENEOUS VERSUS HOMOGENEOUS SURFACE

According to Ozaki, Taylor, and Boudart the concentration of $(NH)_a$ depends upon the H_2 and NH_3 concentrations as indicated in Eq. (4). Desorption of nitrogen from this surface (Eq. 5) is slow and rate-limiting, and does not disturb the equilibrium concentration of $(NH)_a$. Thus, following Langmuir (*10*)

$$A_a e^{-E_a/RT}(NH_3)(1 - \theta_{NH}) = A_d e^{-E_d/RT}(H_2)\theta_{NH} \quad (19)$$

where E_a, and E_d are the activation energies for adsorption and desorption, respectively; θ_{NH} is the fraction of the surface covered by (NH) radicals, and A is a pre-exponential factor.

For a homogeneous surface E_a and E_d are independent of coverage, while for a heter-

ogeneous surface E_a and E_d are linear functions of θ:

$$E_a = E_a^0 + \alpha\theta \quad (20)$$

$$E_d = E_d^0 - \beta\theta \quad (21)$$

and

$$-\Delta H_a = E_d - E_a = -\Delta H_a^0 - (\alpha + \beta)\theta \quad (22)$$

where superscript zero represents values at zero surface coverage. The form of the adsorption isotherm, θ_{NH}, depends upon the nature of the surface. For a homogeneous surface, Eq. (19) is solved directly

$$\theta_{NH} = \frac{K[(NH_3)/(H_2)]}{1 + K[(NH_3)/(H_2)]}, \quad (23)$$

where K is the equilibrium constant for reaction (4). Following Ozaki *et al.* (*6*, *10*b), the isotherm for a heterogeneous surface becomes

$$\theta_{NH} = \frac{2}{f} \ln \frac{1 + K_1^0[(NH_3)/(H_2)]}{1 + K_1^0 e^{-f/2}[(NH_3)/(H_2)]} \quad (24)$$

where $f = \gamma/RT$, $\gamma = \alpha + \beta$, and K_1^0 is the equilibrium constant for reaction (4) at zero coverage.

Similarly, the expression for the rate of desorption of nitrogen depends upon the nature of the surface. In general,

$$r_d = k_d \theta_{NH}^2 e^{-E_d/RT} \quad (25)$$

For a homogeneous surface, E_d is constant so that Eq. (25) becomes

$$r_d = k_d^{I} \theta_{NH}^2 \quad (26)$$

For a heterogeneous surface

$$r_d = k_d \theta_{NH}^2 e^{-E_d^0/RT} e^{\beta\theta/RT} \quad (27)$$

or,

$$r_d = k_d^{II} \theta_{NH}^2 e^{h\theta} \quad (28)$$

where $h = \beta/RT$. For sufficiently heterogeneous surfaces (large β) the exponential term dominates the function, and Eq. (28) can be written

$$r_d \cong k_d^{III} e^{h\theta} \quad (29)$$

Substitution of Eq. (23) into Eq. (26) yields the rate expression for ammonia decomposition on a homogeneous surface, while substitution of Eq. (24) into Eq. (29) yields the expression for decomposition on a heterogeneous surface

$$r_d^{(\text{homogeneous surface})} = k_d^{I} \left[\frac{K[(NH_3)/(H_2)]}{1 + K[(NH_3)/(H_2)]} \right]^2 \quad (30)$$

$$r_d^{(\text{heterogeneous surface})} = k_d^{III} \left[\frac{1 + K_1^0[(NH_3)/(H_2)]}{1 + K_1^0 e^{-f/2}[(NH_3)/(H_2)]} \right]^{2h/f} \quad (31)$$

Assuming for a heterogeneous surface (*6*) that

$$K_1^0[(NH_3)/(H_2)] \gg 1 \gg K_1^0 e^{-f/2}[(NH_3)/(H_2)]$$

then

$$r_d^{(\text{heterogeneous surface})} \approx k_d^{IV}[(NH_3)^2/(H_2)^2]^{1-\delta} \quad (32)$$

where $1 - \delta = h/f$, and $k_d^{IV} = k_d^{III} K_1^0$.

The form of Eqs. (32) or (31) is not the same as that of Eq. (30), as was the case for the analogous equations derived for ammonia syntheses by Ozaki, Taylor, and Boudart (*6*).

The data from the copper and Hastelloy C (No. 3) tube were refitted to Eq. (30). In these calculations estimates were only obtained for parameters in the linear approximation of the equation. However, as indicated from previous experience, the approximation should be good due to the relatively low conversions in the tubes, and they adequately indicate the relative goodness of fit of the data to the two models. Table 4 presents the results for Hastelloy C and copper. An approximate statistical test, based on the Williams and Kloot procedure (*11*), was used to determine whether the apparent model preferences were strong enough to be meaningful. From the residual mean squares, it is indicated that the copper data is fitted better by the homogeneous surface model, while the Hastelloy C data conforms better to the heterogeneous surface model. In both cases the apparent preference is highly significant (the F statistics computed to test the hypoth-

TABLE 4
HETEROGENEOUS VS HOMOGENEOUS SURFACE MODELS FOR COPPER AND HASTELLOY C

	Heterogeneous model (Eq. 7)		Homogeneous model (Eq. 30)	
	Copper (Tube 2)	Hastelloy C (Tube 3)	Copper (Tube 2)	Hastelloy C (Tube 3)
Parameters				
C	0.2533×10^6	17.61×10^6	22.24×10^6	270.7×10^6
E	42 190	41 970	42 450	43 560
m	1.03	0.479	—	—
n	1.02	0.485	—	—
K	—	—	0.06	0.25
Residual sum of squares	2.303	0.0667	1.617	0.101
Degrees of freedom	18	18	19	19
Residual mean square	0.128	0.00371	0.085	0.00531

esis of no preference exceeded the 99.9% significance level).

These data indicate that the copper surface, although certainly not entirely homogeneous, may be more homogeneous than the alloy surfaces. In other words, the f value (change in heat of adsorption with coverage) for copper is not large enough so that the term $K_1^0 e^{-f/2}$ $[(NH_3)/(H_2)]$ in Eq. (31) is negligible compared to one.

The validity of the assumption that K_1^0 $[(NH_3)/(H_2)] \gg 1$ is not determined. The data were not sufficient to correlate it according to Eq. (31), which contains five parameters (including the temperature dependency of k_d^{III}).

EFFECT OF NITROGEN

The effect of nitrogen on the kinetics of ammonia decomposition was determined by performing four sets of paired experiments with excess nitrogen and argon added to the feed stream. Each paired experiment was done at approximately the same temperature level and NH_3 and H_2 concentrations, the difference being that in one case excess N_2 (above that present from NH_3 precracking) was present, and in the second case argon (equivalent to the excess N_2) was present. The increase in hydrogen in each case was then observed, and the ammonia decomposition rates were compared.

In comparing the rates for the various cases, differential behavior in the tubes was assumed. That is, the rates were described by Eqs. (11) and (12); and the average temperatures, and partial pressures by Eqs. (13)–(15). Since the conditions in each paired experiment were not exactly equivalent with respect to temperature and NH_3 and H_2 partial pressures, the observed linear rates were corrected according to Eq. (18). That is

$$\frac{r_A}{r_N} = \exp(\ln y_A - \ln y_N) \exp\left(\frac{E}{R\bar{T}_A} - \frac{E}{R\bar{T}_N}\right) \left(\frac{\bar{P}_{NH_3-N}}{\bar{P}_{NH_3-A}} \frac{\bar{P}_{H_2-A}}{\bar{P}_{H_2-N}}\right)^m \quad (33)$$

where r is the corrected linear decomposition rate, y the observed rate $(\Delta A'/2\pi rl)$, and the subscripts A or N refer to the argon case and nitrogen case, respectively.

The results of these experiments are presented in Table 5, and indicate that nitrogen has no effect on the kinetics of ammonia decomposition. The ratios of decomposition rates show no positive tendency of nitrogen inhibition. Especially revealing is the result that the rate ratios of Experiment IV, which always has the highest ratio of argon to nitrogen, are not significantly different from rate ratios of experiments with less or no argon present. Deviations from the ideal rate ratio of one (no effect of nitrogen) are attributed to errors in assuming differential decomposition rates, and errors in the thermal conductivity cell calibration due to the presence of four components.

TABLE 5

RELATIVE EFFECTS OF NITROGEN AND ARGON ON DECOMPOSITION RATE

Experiment	$\bar{P}_{NH_3}$ (psi)	$\bar{P}_{H_2}$ (psi)	$\bar{P}_A$ (psi)	$\bar{P}_{N_2}$ (psi)	Average tube Temp. $\bar{T}$ (°K)	Ratio of observed rates (corrected for differences in temperature and $NH_3 + H_2$ partial pressures) r_A/r_N
Tube 2—Copper (E = 42.5 kcal/mole)						
I. a. Argon dilution	15.9	3.77	7.62	1.26	989.8	0.984
b. Nitrogen dilution	15.8	3.74	0	8.21	992.0	
II. a. Argon dilution	16.0	2.46	10.21	0.82	997.9	1.17
b. Nitrogen dilution	15.3	1.84	0	10.03	991.7	
III. a. Argon dilution	16.5	2.79	7.79	0.93	887.6	1.02
b. Nitrogen dilution	15.5	2.53	0	8.01	884.8	
IV. a. Argon dilution	17.1	0.804	9.82	0.28	883.9	1.13
b. Nitrogen dilution	16.0	0.734	0	9.38	884.6	
Tube 5—Hastelloy C (E = 44.2 kcal/mole)						
I. a. Argon dilution	15.0	4.52	7.40	1.51	977.9	1.21
b. Nitrogen dilution	15.0	3.92	0	8.72	979.1	
II. a. Argon dilution	14.9	3.44	9.98	1.15	985.1	1.19
b. Nitrogen dilution	14.4	2.58	0	10.08	978.8	
III. a. Argon dilution	16.3	2.86	7.78	0.95	882.1	0.88
b. Nitrogen dilution	15.3	2.61	0	8.11	879.5	
IV. a. Argon dilution	16.9	0.978	9.68	0.326	877.2	1.12
b. Nitrogen dilution	15.7	0.886	0	9.41	877.9	
Tube 4—Inconel (E = 40.0 kcal/mole)						
I. a. Argon dilution	14.1	5.3	7.26	1.77	972.1	1.19
b. Nitrogen dilution	14.2	4.63	0	8.81	973.0	
II. a. Argon dilution	13.9	4.25	9.8	1.42	978.1	1.11
b. Nitrogen dilution	13.6	3.36	0	10.10	972.5	
III. a. Argon dilution	16.1	3.05	7.72	1.02	880.8	0.94
b. Nitrogen dilution	15.0	2.78	0	8.24	878.4	
IV. a. Argon dilution	16.6	1.29	9.57	0.43	875.6	1.095
b. Nitrogen dilution	15.3	1.156	0	9.54	876.5	

ACKNOWLEDGMENTS

The authors wish to thank L. C. Beegle for his help in the design and construction of the apparatus, S. Kern for her role in the writing and execution of the computer program, E. J. Thomas for the photomicrographs, J. Smith for his help in collection of the data, and finally F. DeMaria and J. E. Longfield for many helpful discussions.

REFERENCES

1. TEMKIN, M., AND PYZHEV, V., *Acta Physicochem. URSS* **12**, 327 (1940).
2. (a) ENOMOTO, S., AND HORIUTI, J., *J. Res. Inst. Catalysis, Hokkaido Univ.* **2**, 87 (1953); (b) ENOMOTO, S., HORIUTI, J., AND HOBAYASHI, H., *ibid.* **3**, 185 (1955); (c) HORIUTI, J., AND TOYOSHIMA, I., *ibid.* **5**, 120 (1957); **6**, 58

(1957); (d) HORIUTI, J., *J. Catalysis* **1**, 199 (1962).

3. LOVE, K., AND EMMETT, P. H., *J. Am. Chem. Soc.* **63**, 3297 (1941).
4. EMMETT, P. H., "New Approaches to the Study of Catalysis," Thirty-sixth Annual Priestly Lecture, Pennsylvania State University, University Park, Pa., 1962, pp. 91–120.
5. BORKHOVEN, C., GORGELS, M. J., AND MARS, P., *Trans. Faraday Soc.* **55**, 315 (1959).
6. OZAKI, A., TAYLOR, H. S., AND BOUDART, M., *Proc. Roy. Soc. (London)* **A258**, 47 (1960).
7. ANDERSON, R. L., AND BANCROFT, T. A., "Statistical Theory in Research." McGraw-Hill, New York, 1952.
8. HILDEBRAND, F. B., "Introduction to Numerical Analysis." McGraw-Hill, New York, 1956.
9. (a) BOX, G. E. P., *Ann. N. Y. Acad. Sci.* **86**, 792 (1960); (b) "Non-Linear Estimation (Princeton—I.B.M.) 704 Program WLN *LT*," Mathematics and Applications Dept., IBM Corp., New York, 1959.
10. (a) LANGMUIR, I., *J. Am. Chem. Soc.* **40**, 1361 (1918); (b) BRUNAUER, S., LOVE, K., AND KENNAN, R., *ibid.* **64**, 751 (1942).
11. WILLIAMS, E. J., "Regression Analysis." Wiley, New York, 1959.